

Hans Essone Obame
Arsène Eya'a Mvongbote
Honoré Gnanga

Laboratoire Pluridisciplinaire des
Sciences (LAPLUS),
Ecole Normale Supérieure,
Libreville, GABON



Experimental and Modeling of a Photovoltaic Panel Efficiency under Equatorial Africa Conditions: Influence of Relative Humidity (RH) and Temperature

Variation of the photovoltaic panels' performance caused by severe environmental conditions requires precise characterization of electrical behavior dependence of this material with these atmospheric conditions. This article presents environmental causes, in the equatorial Africa region, especially in Gabon, Libreville city, of solar panels failure then presents results from an experimental study (thanks to an in situ characterization bench of photovoltaic solar panels) and a simulation model to predict the efficiency of a system photovoltaic (PV) operating in harsh environmental conditions such as an atmosphere of $\geq 80\%$ of relative humidity (RH) and temperature up to $40\text{ }^{\circ}\text{C}$ and thus know the performance of these electrical components. The objective of this paper is centered on the power and fill factor, which is affected by parasitic (shunt) resistance, depending on open-circuit voltage (V_{oc}) and short circuit (I_{sc}) current with the help of the MATLAB model and experimental data. Results are discussed.

Keywords: PV Cell Model; Electrical Contact; Shunt Resistance; Equatorial Atmosphere
Received: 10 October 2023; **Revised:** 13 November; **Accepted:** 20 November 2023

1. Introduction

The demand for renewable energy sources has increased to meet energy demand using conventional systems [1,2]. The continued use of fossil fuels has led to a reduction in fossil fuel deposits and has significantly impacted the environment, affecting the biosphere and contributing to global warming.

In equatorial Africa, solar energy is abundant and can be harvested and used efficiently [3]. Solar energy can be used as a standalone generating unit or a grid-connected unit, depending on the availability of a nearby grid.

Another advantage of using solar energy is the easy access to portable operation wherever needed. The power mechanisms have been significantly reduced in size over the recent past years. Photovoltaic modules (PV) are the main component of a solar energy generation system.

In PV applications, some equipment may contain components that are highly sensitive to environmental conditions. One of the drawbacks of PV is their sensitivity to extreme environmental conditions, such as those found in equatorial Africa [3,4]. By understanding how these unregulated environmental factors affect the component and using this knowledge in the design phase, equipment reliability can be improved, reducing failures and maintenance costs. Some studies have shown an

aging correlation between relative humidity HR (%) and temperature T [5-9].

The authors of a study conducted in Gabon simulated the mathematical modeling of a PV module using Matlab and analyzed characteristics such as voltage-current (V-I) and power-voltage (P-V) for different parameters such as irradiances, temperatures, relative humidity, and shunt resistance. This study is the first to compare simulation results with those of measurements made in real situations on solar panels in Gabon.

Characterizations under natural light must be made only when the light does not fluctuate by more than 1% during the measurement. According to standard IEC 60904-1, the following instrumentation is required:

A calibrated reference cell (60904-2) or a pyranometer, or a luxmeter, measuring the irradiance received.

Temperature sensors (for the reference cell and the cell tested) whose measurement has an uncertainty of less than $\pm 1\%$ and a repeatability of ± 0.5 .

The V_{oc} and I_{sc} measurements must have an accuracy of 0.2% and make in 4 wires.

For the experimental setup, the current-voltage characteristics of the PV module were measured via a variable load (resistance), from zero (short circuit)

to infinity (open circuit). It is possible to vary in the decreasing direction, from V_{oc} to I_{sc} , or in the increasing direction, from I_{sc} to V_{oc} .

Simultaneously, the overall horizontal irradiance was measured by a luxmeter (PM6612L model), and a thermometer-hygrometer reads the values of the temperature and relative humidity.

A database has been implemented, and a SigmaPlot® program allows easy access to the data and the associated mathematical processing.

Nomenclature

- I the output current of PV cell
- V the output voltage of PV cell
- I_{ph} the photocurrent
- I_0 the reverse saturation current of diode
- V_d the diode voltage
- I_d the diode current
- I_0 the reverse saturation current of diode
- a the diode ideality factor
- k the Boltzmann constant
- T the p-n junction temperature
- q the electron charge
- K_i short-circuit current/temperature coefficient
- K_v open-circuit voltage/temperature coefficient
- G actual sun irradiation
- G_{STC} nominal sun irradiation (690 W/m²)
- $I_{ph,STC}$ nominal photocurrent (25°C and 690W/m²)
- N_s the number of cells connected in series
- V_{oc} open circuit voltage
- I_{sc} short circuit current
- FF fill factor

2. PV Cell Model

The equivalent circuit of a photovoltaic cell consists of a current source and a diode connected in parallel, as shown in Fig. (1). This model also includes a series resistance and a shunt resistance [10]. The equation that describes this model is given below

$$I = I_{ph} - I_0 \left(\exp\left(\frac{aV_d}{kT}\right) - 1 \right) \tag{1}$$

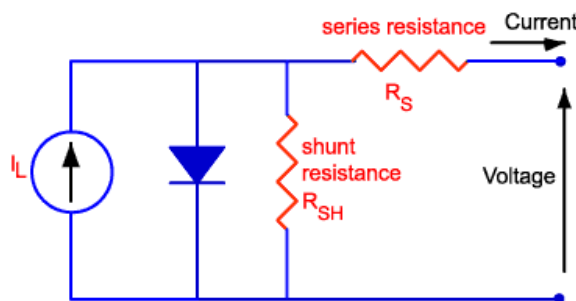


Fig. (1) The equivalent circuit of a solar cell

The single diode model includes the series resistance R_s and shunt resistance R_p (or R_{sh}), where the output current can be written as ^(10, 11, 12).

$$I = I_{ph} + I_0 \left(\exp\left(\frac{V+IR_S}{aV_T}\right) - 1 \right) - \frac{V+IR_S}{R_{sh}} \tag{2}$$

The photocurrent, which is the current produced by the photovoltaic cell when it absorbs sunlight, is determined by the solar insolation and the cell's working temperature. The expression for the photocurrent is given by [11,12]:

$$I_{ph} = (I_{ph,STC} + K_I \cdot \Delta T) \cdot \frac{G}{G_{STC}} \tag{3}$$

and the reverse saturation current

$$I_0 = \frac{I_{ph,STC} + K_I \Delta T}{\exp\left(\frac{V_{oc,STC} + K_V \Delta T}{aV_T}\right) - 1} \tag{4}$$

The Fill Factor (FF) is a crucial parameter of a solar cell that determines the maximum power output. It is defined as the ratio of the maximum power point to the product of V_{oc} and I_{sc} . PV panels usually have an FF ranging from 0.4 to 0.8, while the FF of ideal PV panels is 1.0. The FF is a measure of the "squareness" of the I-V characteristic of the solar cell [2]

$$FF = \frac{P_{max}}{V_{oc} I_{sc}} \tag{5}$$

3. PV Cell Performance with different parameters

3.1. Details of data including Relative Humidity (RH), temperature and insolation for Libreville, Gabon

Relative humidity

Libreville latitude 0.393 longitudes 9.454. Table (1) contains all months corresponding to their average relative humidity [13].

There are two scenarios to consider when analyzing the effect of moisture. One is how water vapor particles affect the irradiation level of sunlight and the other is how humidity enters the solar cells' enclosure [5].

Figure (2) shows that irradiance decrease with increasing RH.

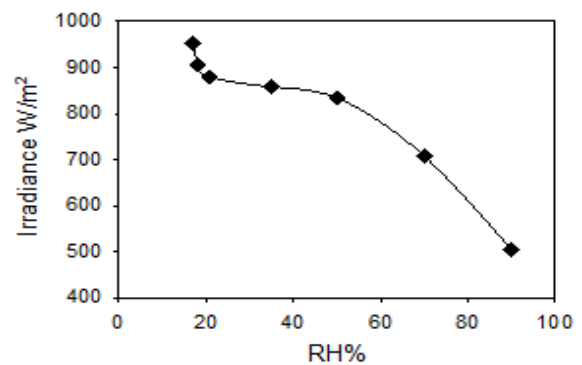


Fig. (2) Irradiance level with respect to relative humidity [5]

Moisture ingress through adsorption, primarily driven by humidity, exerts a significant influence on the performance of solar cells. In the second approach, we examine how humidity affects the efficiency of solar cells, particularly through the moisture ingress via the adsorption process [6]. Prolonged exposure to humidity has been observed to lead to a deterioration in solar cell performance. For instance, the presence of high levels of water vapor

in the surrounding air can result in encapsulant delamination. The extended exposure of photovoltaic cells to humidity is associated with several performance degradations. Notably, the abundance of water vapor in the air has been linked to encapsulant delamination [7], subsequently causing a reduction in parallel resistance [14], as illustrated in the accompanying graph [15]. The systematic decline in sheet resistance can be observed across various samples as relative humidity increases, as depicted in Fig. (3).

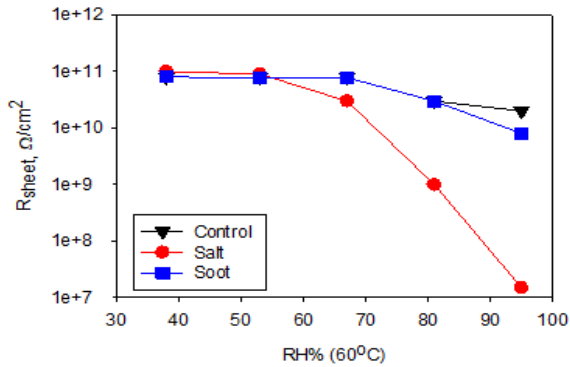


Fig. (3) Sheet resistance of various soils as on glass and an unsoiled control as a function of relative humidity at 60°C [16]

Temperature

Table (2) contains all months corresponding each to their average temperature [13].

Irradiance

Table (3) contains all month corresponding respectively to their average insolation [13].

3.2. Resistances

Series resistance (Rs)

Series resistance is due to the contribution of base resistors and the front of the junction and the front and rear contacts. The series resistance effect is very small (a few mΩ).

Shunt resistance (Rsh)

The parallel (shunt) resistance plays a critical role in addressing issues such as current leakage along the edges of the solar cell. This resistance is diminished when metal impurities infiltrate the junction, particularly if this infiltration extends deep into the cell structure. The impact of parallel resistance is primarily associated with the manufacturing process and is most pronounced when dealing with extremely low current values, typically in close proximity to the short-circuit current [16].

Figure (4) shows the method of measuring shunt resistance.

3.3. Studied PV module

Studied model characteristics are given in table (4).

Below (Fig. 5), the experimental bench was used to measure the electrical parameters of the studied solar panel.

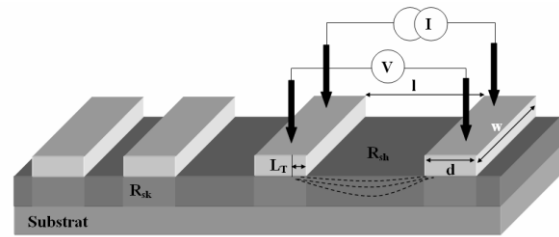


Fig. (4) Resistance measurement [15]

Table (4) Schneider AEH-LP01-SBG-5W typical electrical characteristic

| Output (Wp) | Size (mm) | Weight (Kgm) | Pmax (W) | Vmp (V) | Imp (A) | Voc (V) | Isc (A) |
|-------------|----------------|--------------|----------|---------|---------|---------|---------|
| 5 | 306 x 218 x 25 | 1.0 | 5 | 16.8 | 0.3 | 21 | 0.39 |



Fig. (5) Experimental bench

4. Results and discussion of Matlab™ model of the PV Module

4.1 Constant temperature (25°C) with different irradiation

In all three models, the temperature is maintained at a constant 25 °C, while the irradiation levels are varied (100 W/m², 360 W/m², and 690 W/m²). Figure (6) displays the results obtained using the Matlab™ program under these conditions, showcasing the I-V and P-V characteristics, respectively. The current generated by incident light is inherently linked to the irradiation level, with higher irradiation leading to greater current production. Conversely, the voltage experiences a decrease of 3 V as solar radiation increases from 100 to 690 W/m². The impact of irradiation on the maximum power point is evident, with higher irradiation resulting in a higher maximum power point, reaching 6.74 W.

As depicted in Fig. (6), it is evident that the electrical parameters of the solar cells, including Isc (short-circuit current), Voc (open-circuit voltage), Pmax (maximum power), and FF (fill factor), are influenced by the level of illumination.

As illustrated in Fig. (7), the current produced by the photovoltaic (PV) cell is significantly influenced by solar radiation. The Schottky equation highlights the dependency of both Isc (short-circuit current) and Voc (open-circuit voltage) on the intensity of light. The short-circuit current experiences a linear increase with rising light intensity, attributed to the enhanced photon-to-current conversion rate. In accordance

with the energy state distribution within the semiconductor, the open-circuit voltage also shows a proportional increase. Similarly, the maximum current, P_{max} , exhibits a linear rise, as depicted in Fig. (7a). The maximum power point, P_{max} , also follows a linear increase in response to light intensity, as shown in Fig. (7a).

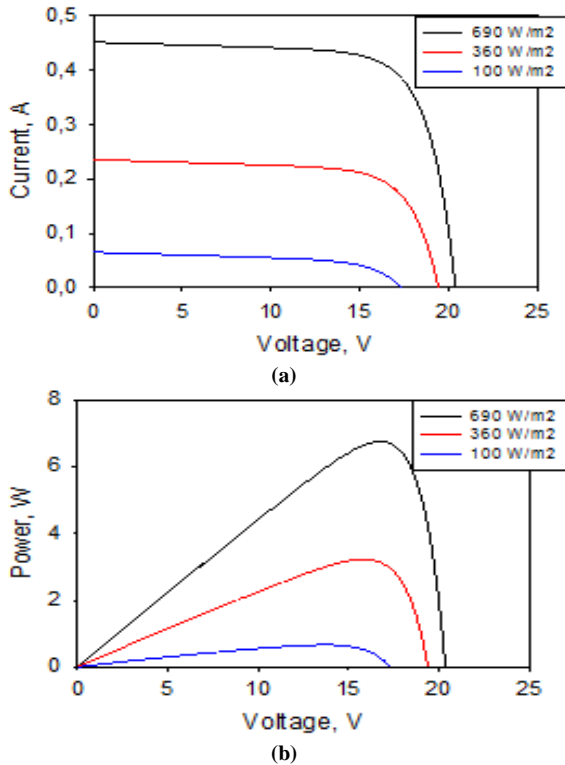


Fig. (6) (a) I-V characteristics of the panel, at 25° C for different irradiance levels, and (b) P-V characteristics of the panel, at 25° C for different irradiance levels

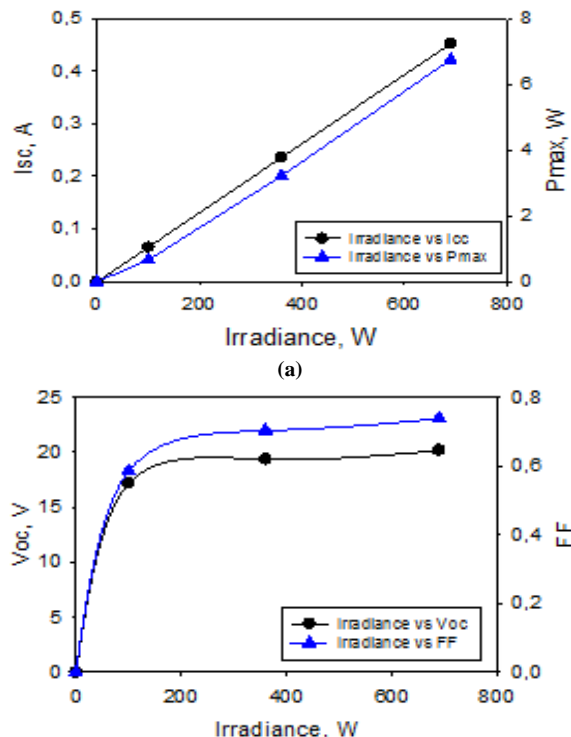


Fig. (7) (a) Dependency of the solar cell I_{sc} on illumination levels, at 25 °C, and (b) Dependency of the solar cell V_{oc} on illumination levels, at 25 °C

Nonetheless, the inherent internal resistance of the cell and the shunt resistance within the circuit serve as constraining factors, preventing the fill factor (FF) of the PV cell from reaching its ideal value of 1, as depicted in Fig. (7b).

4.2. Constant irradiation with different temperature

Figure (8) illustrates the impact of temperature on the I-V characteristics of the solar cell as temperature varies. An increase in temperature results in a corresponding rise in the short-circuit current (I_{sc}) while concurrently causing a notable decrease in the open-circuit voltage (V_{oc}). The curves demonstrate I_{sc} changes from 0.45 to 0.475A as the temperature shifts from 25 to 45°C. This temperature elevation leads to a decrease in voltage (V_{oc}), from 20.4 to 17 V, along with a slight increase in current (I_{sc}), followed by a relative decrease in maximum power (P_{max}).

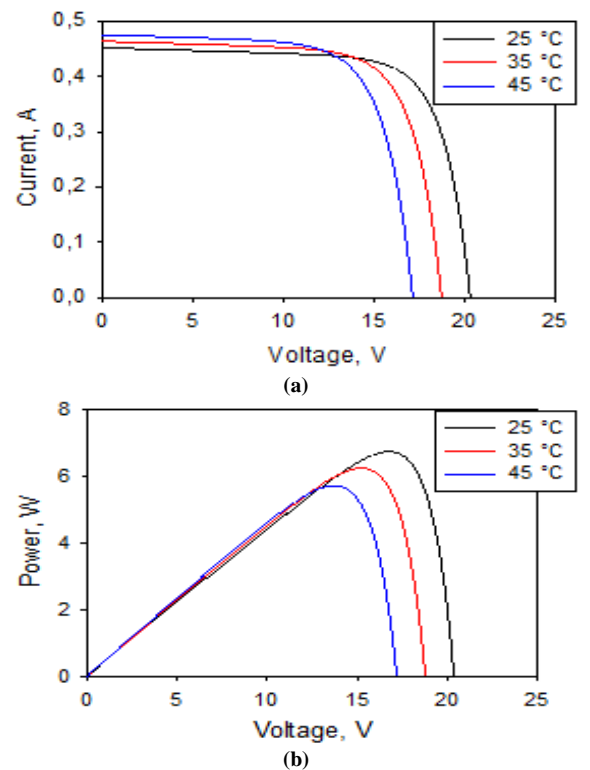


Fig. (8) (a) I-V characteristics for different temperatures but same light intensity 690 W/m², and (b) P-V characteristics for different temperatures but same light intensity 690 W/m²

The key cell parameters are graphed as functions of temperature in Fig. (9), under constant light intensity conditions. A temperature-dependent relationship becomes evident. In this figure, the open-circuit voltage is depicted as a function of temperature with constant light intensity (690 W/m²). The exponential dependence of the saturation current

on temperature leads to a rapid decline in the open-circuit voltage as temperature rises. The same figures also show that power output decreases with increasing temperature, and the fill factor (FF) exhibits a similar trend. At room temperature, FF is 0.74, but this value decreases to 0.705 at 45°C.

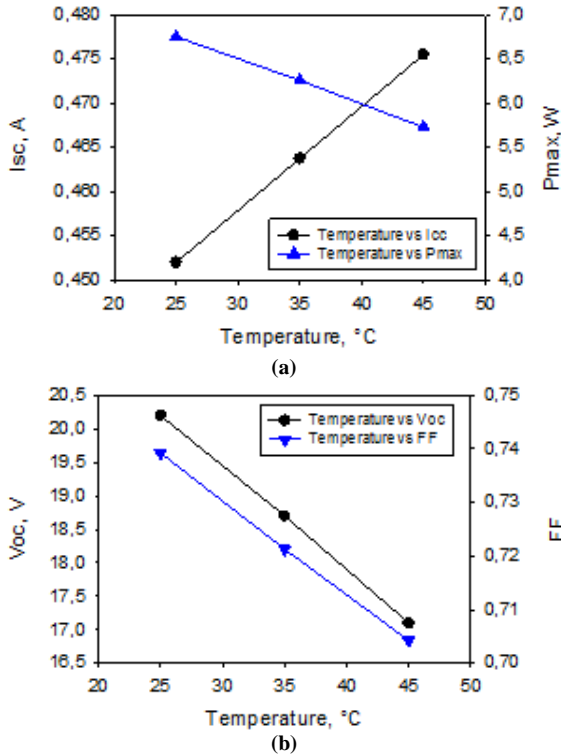


Fig. (9) (a) Calculated I_{sc} and P_{max} as functions of temperature, light intensity = 690 W/m², and (b) Calculated V_{oc} and FF as functions of temperature, light intensity = 690 W/m²

4.3. Variation of shunt resistance

Figure (10) below depicts the impact of shunt resistance (R_{sh}) on the I-V characteristics of a solar cell under identical illumination conditions. The presence of shunt resistance influences these characteristics, leading to a slight reduction in the open-circuit voltage and an increase in the slope of the I-V curve within the region corresponding to the cell's operation as a current source (low voltage).

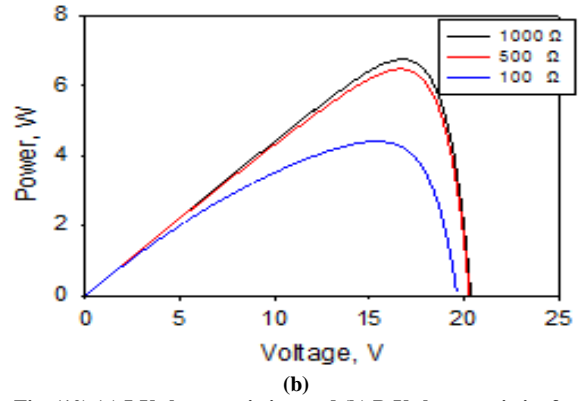
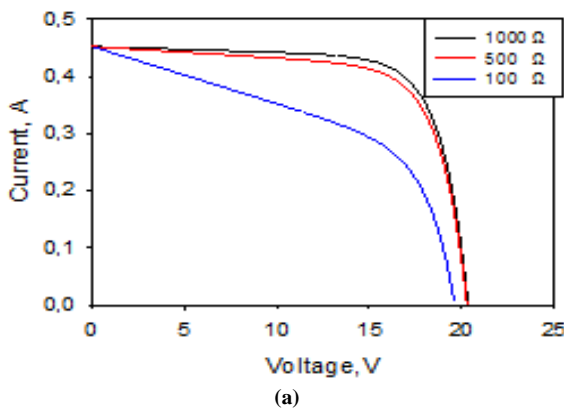


Fig. (10) (a) I-V characteristics, and (b) P-V characteristics for different shunt resistance values

The electrical parameters of the cell as functions of shunt resistance are presented in Fig. (11). In this scenario, the temperature remained constant at 25°C, while the light intensity remained at 690 W/m². Decreasing the shunt resistance has an overall effect on reducing the voltage value.

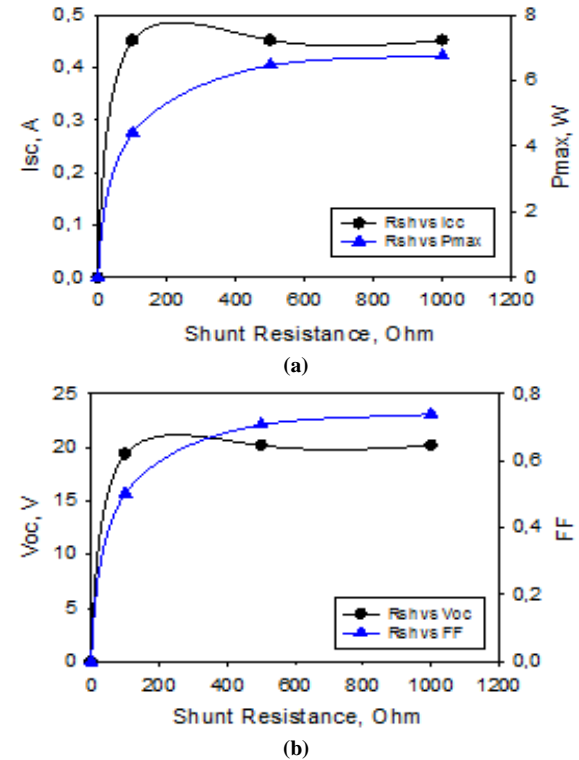


Fig. (11) (a) Calculated I_{sc} and P_{max} as functions of resistance (R_{sh}), and (b) Calculated V_{oc} and FF as functions of resistance (R_{sh}), light intensity is 690 W/m² at ambient temperature of 25°C

Both the fill factor (FF) and the maximum power decrease as R_{sh} decreases, as illustrated in Fig. (11). Notably, when R_{sh} decreases significantly, V_{oc} also experiences a significant decrease. These figures further reveal that for relatively small values of R_{sh} , the light-generated current takes an alternative path, resulting in power loss. When R_{sh} is large but still smaller than 5 Ω, I_{sc} , V_{oc} , P_{max} , and FF remain

relatively constant. These findings align with those reported in existing literature [17,18].

4.4. Comparison between Mathematical Model and Experimental Data

Figure (12) presents data obtained in ambient conditions, ranging from 425 W/m² and 42°C to 425 W/m² and 34°C. Subsequently, a comparison is made with the simulation results derived from the equations described earlier. In the experiment conducted at 34°C, a maximum power of 7.12 W was achieved, in contrast to the 5 W obtained in the simulation. The short-circuit current reached 0.56 A, as opposed to the simulated 0.39 A, and the open-circuit voltage was 19.8 V instead of the simulated 21.6 V. In the experiment at 42°C, the values of short-circuit current, power, and open-circuit voltage were lower, at 0.47 A, 6.5 W, and 19.15 V, respectively. These findings align with results documented in the existing literature [19-22].

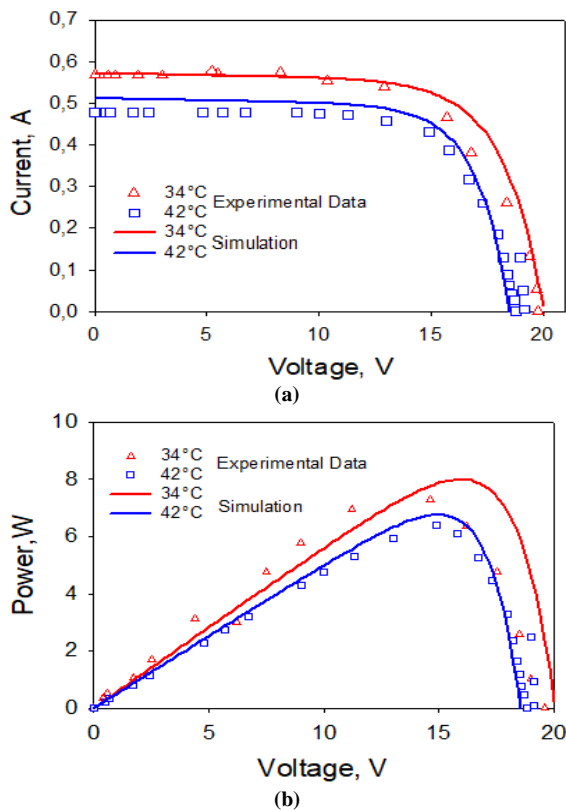


Fig. (12) I-V characteristics (a) and P-V characteristics (b) for experimental results and mathematical treatment

These results serve to validate the appropriateness of the laws proposed in our single-diode model for accounting for losses. Discrepancies between experimental values and the model may arise from unaccounted parameters such as relative humidity and variations in the solar spectrum during the simulation.

The outcomes of this study underscore the challenge of establishing "external STC (Standard Test Conditions)" that would facilitate fair comparisons of different photovoltaic modules.

Consequently, it becomes imperative to identify criteria for evaluating PV performance under real-world conditions, such as the performance ratio (PR), defined as the ratio between the actual yield in operational scenarios and the yield under STC.

4.5. Variation of Relative Humidity (RH)

Given the unavailability of a humidity-linked numerical model, we conducted an experimental investigation into the impact of humidity on the panel's performance.

Figure (13) illustrates the variations in I_{sc} (short-circuit current) and V_{oc} (open-circuit voltage) relative to relative humidity (RH). The measurements were taken under irradiance ranging from 583 to 690 W/m² and temperatures between 25 and 30°C. Notably, both I_{sc} and V_{oc} exhibit a decrease as RH levels increase. This decline can be attributed to the fact that high relative humidity can contribute to solar irradiance in three distinct ways: diffraction, reflection, and absorption. Consequently, these results underscore the detrimental effect of relative humidity on the performance of the photovoltaic panel. It is important to acknowledge that irradiance and temperature also play a role, although in our test conditions, their variations were minimal, and their changes were not necessarily linked to changes in relative humidity.

These findings align with the results obtained by Panjwani in 2014 [23], Kazem in 2015 [24], and Bonkaney in 2017 [25].

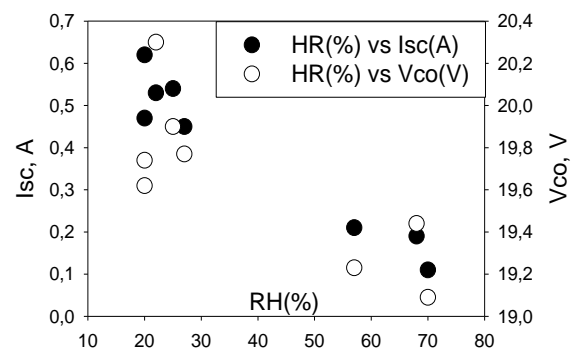


Fig. (13) Dependency of solar panel parameters (I_{sc} and V_{oc}) on relative humidity (RH), plotted at light intensity between 583 and 690 W/m² and ambient temperature from 25 to 30°C

5. Conclusion

We have developed an accurate electrical model for a PV module based on a simple one-diode mathematical framework, and this model has been demonstrated using Matlab™ for a representative 5 W solar panel. The proposed model was employed to assess the impact of sunlight irradiance across various equatorial situations in Africa, utilizing input and output parameters related to I-V and P-V characteristics, cell temperature, and shunt resistance. The Matlab results exhibit a remarkable alignment with the manufacturer's published data.

Given the prevailing conditions in the region, characterized by relatively low irradiance levels (less than 700 W/m^2), high relative humidity, and an average temperature of up to 25°C , optimizing the efficiency of this photovoltaic module necessitates the maintenance of a high shunt resistance, ideally up to 1000Ω . These initial findings on relative humidity are promising, suggesting the potential for future research to conduct a statistical study on the influence of this parameter on a panel's electrical performance. This could lead to the development of mathematical models that specifically account for moisture-related effects.

References

- [1] T. Huan-Liang, T. Ci-Siang and S. Yi-Jie, "Development of Generalized Photovoltaic Model Using Matlab/Simulink", Proc. World Cong. on Eng. Computer Sci. (San Francisco, USA) (2008).
- [2] S.R. Sinsel, R.L. Riemke and V.H. Hoffmann, "Challenges and solution technologies for the integration of variable renewable energy sources—a review", *Renew. Ener.*, 145 (2020) 2271-2285
- [3] V.B. Omubo-Pepple, I. Tamunobereton-Ari and M.A. Briggs-Kamara, "Influence of meteorological parameters on the efficiency of photovoltaic module in some cities in the Niger delta of Nigeria", *J. Asian Sci. Res.*, 3(1) (2013) 107-113.
- [4] L. Apicella, L. Egiziano and V. Nicolais, "Environment degradation of electrical and thermal properties of organic insulating materials", *J. Mater. Sci.*, 23 (1988) 729-735.
- [5] G. Bal and D. Creasey. "Humidity: a factor in the appropriate positioning of a photovoltaic power station", *Renew. Ener.*, 6(3) (1995) 313-316.
- [6] S. Mekhilef, R. Saidur and M. Kamalisarvestani, "Effect of dust, humidity and air velocity on efficiency of photovoltaic cells", *Renew. Sustain. Ener. Rev.*, (16) (2012) 2920-2925.
- [7] H. Conseil et al., "Humidity Buildup in Electronic Enclosures Exposed to Constant Conditions", *IEEE Trans. Comp. Packag. Manufact. Technol.*, 7(3) (2017) 412 - 423.
- [8] Y. Yao et al., "The effect of ambient humidity on the electrical properties of graphene oxide films", *Nanoscale Res. Lett.*, (7) (2012) 363.
- [9] S.K. Singh, S.K. Biswal and N. Pal, "Environmental impact on solar photovoltaic module and its detail analysis for different varying parameters", *Int. J. Ind. Electron. Elect. Eng.*, 2(6) (2014) 15-19.
- [10] M. Azzouzi and M. Stork, "Modeling and simulation of a photovoltaic cell Considering single-diode model", *Int. J. Res. Eng. Technol.*, 2(11) (2014) 19-28.
- [11] N. Sultana, A. Ahad and Md. Kamrul Hassan, "Simulation and Analysis of the Effect of Change of Different Parameters on the Characteristics of PV Cell Using LTspiceIV", *Int. J. Sci. Res.*, 4(2) (2015) 63-68.
- [12] F.M. González-Longatt, "Model of Photovoltaic Module in Matlab™", *2^{do} Congreso iberoamericano de estudiantes de ingeniería eléctrica, electrónica y computación (Cibelec)* (Venezuela), (2005) pp. 1-5.
- [13] Atmospheric Science Data Center [Online], available at: <https://eosweb.larc.nasa.gov/cgi-bin/sse/grid.cgi?email=skip@larc.nasa.gov>. [Accessed: Jul.2, 2018]
- [14] P. Hacke et al., "Effects of Photovoltaic Module Soiling on Glass Surface Resistance and Potential-Induced Degradation", *Proc. 43rd IEEE Photovol. Special. Conf.*, New Orleans, Louisiana (2015) pp. 14-19.
- [15] D. Schröder and D. Meier, "Solar cells contact resistance: a review", *IEEE Trans. Electron Dev.*, 31(5) (1984) 637-647.
- [16] D. Meier and D. Schröder, "Contact resistance: its measurement and relative importance to power loss in a solar cell", *IEEE Trans. Electron Dev.*, 31(5) (1984) 647-653.
- [17] A.D. Dhass, E. Natarajan and L. Ponnusamy, "Influence of Shunt Resistance on the Performance of Solar Photovoltaic Cell", *Int. Conf. Emerg. Trends Elect. Eng. Ener. Manag. (ICETEEEM)* (Chennai, India) (2012) 382-386.
- [18] I.D. Sara, "Effects of Shunt and Series Resistances on the Performance of a Tandem Solar Cell", *Int. Conf. Elect. Eng. Inform. (ICELTICs)*, (Banda Aceh, Indonesia) (2017) 159-162.
- [19] M. Barbato et al., "Influence of Shunt Resistance on the Performance of an Illuminated String of Solar Cells: Theory, Simulation, and Experimental Analysis", *IEEE Trans. Dev. Mater. Reliab.*, 14(4) (2014) 942-950.
- [20] S. Sarikh et al., "Design of an I-V Characteristic Tracer for Photovoltaic Systems", *Int. Renew. Sustain. Ener. Conf. (IRSEC'2017)*, (Tangier, Morocco) (2017) 1-5.
- [21] C. Ikedi, "Experimental Study of Current-Voltage Characteristics for Fixed and Solar Tracking Photovoltaics Systems", in *Recent Developments in Photovoltaic Materials and Devices*, IntechOpen (2019) 128-140.
- [22] Y. Sun et al., "The I -V Characteristics of Solar Cell under the Marine Environment: Experimental Research", *4th Int. Conf. Renew. Ener. Res. Appl.*, Palermo, Italy (2015) 403-408.
- [23] M.K. Panjwani and G.B. Narejo, "Effect of Humidity on the Efficiency of Solar Cell (photovoltaic)", *Int. J. Eng. Res. General Sci.*, 2(4) (2014) 499-503.
- [24] H.A. Kazem, "Effect of Humidity on Photovoltaic Performance Based on Experimental Study", *Int. J. Appl. Eng. Res.*, 10(23) (2015) 43572-43577.

[25] A.L. Bonkaney, S. Madougou and R. Adamou, "Impact of Climatic Parameters on the Performance of Solar Photovoltaic (PV) Module

in Niamey", *Smart Grid Renew. Ener.*, 8 (2017) 379-393.

Table (1) Monthly Averaged relative humidity (%) [13]

| Lat 0.393 Lon 9.454 | Jan | Feb | Mar | Apr | May | Jun | Jul | Aug | Sep | Oct | Nov | Dec | Annual Average |
|---------------------|------|-----|------|------|------|------|-----|------|-----|------|------|------|----------------|
| 22-year Average | 84.9 | 84 | 83.3 | 84.2 | 84.9 | 84.2 | 80 | 74.5 | 79 | 82.3 | 85.3 | 85.8 | 81.9 |

Table (2) Monthly Averaged Air Temperature at 10 m above the Surface of the Earth (°C) [13]

| Lat 0.393 Lon 9.454 | Jan | Feb | Mar | Apr | May | Jun | Jul | Aug | Sep | Oct | Nov | Dec | Annual Average |
|------------------------|------|------|------|------|------|------|------|------|------|------|------|------|----------------|
| 22-year Average | 24.9 | 25.3 | 25.6 | 25.6 | 25.3 | 24.2 | 20.8 | 24 | 24.3 | 24.6 | 24.7 | 24.8 | 24.7 |
| Minimum | 23.3 | 23.5 | 23.8 | 24 | 23.7 | 22.4 | 21.6 | 22 | 22.7 | 23.1 | 23.3 | 23.3 | 23 |
| Maximum | 26.7 | 27.3 | 27.7 | 27.4 | 27.1 | 26.1 | 26 | 26.1 | 26.1 | 26.2 | 26.3 | 26.5 | 26.6 |

Table (3) Monthly Averaged Insolation Incident on a Horizontal Surface at Indicated GMT Times (kW/m²)

| Lat 0.393 Lon 9.454 | Jan | Feb | Mar | Apr | May | Jun | Jul | Aug | Sep | Oct | Nov | Dec |
|------------------------|------|------|------|------|------|------|------|------|------|------|------|------|
| Average@06h | 0.06 | 0.05 | 0.06 | 0.07 | 0.07 | 0.07 | 0.06 | 0.06 | 0.07 | 0.08 | 0.08 | 0.07 |
| Average@09h | 0.46 | 0.48 | 0.49 | 0.46 | 0.44 | 0.44 | 0.43 | 0.47 | 0.49 | 0.44 | 0.41 | 0.45 |
| Average@12h | 0.69 | 0.69 | 0.69 | 0.65 | 0.61 | 0.60 | 0.61 | 0.61 | 0.59 | 0.52 | 0.56 | 0.65 |
| Average@15h | 0.40 | 0.44 | 0.42 | 0.39 | 0.36 | 0.32 | 0.33 | 0.32 | 0.33 | 0.34 | 0.33 | 0.35 |
| Average@18h | 0.01 | 0.02 | 0.01 | 0.01 | 0.01 | 0.01 | 0.01 | 0.01 | 0.01 | 0.00 | 0.00 | 0.01 |